Supplement of Atmos. Chem. Phys., 24, 6787–6807, 2024
https://doi.org/10.5194/acp-24-6787-2024-supplement

Supplement of

Diagnosing uncertainties in global biomass burning emission inventories and their impact on modeled air pollutants

Wenxuan Hua et al.

Correspondence to: Sijia Lou (lousijia@nju.edu.cn)

S1. Biomass Burning emission inventories

S1.1 Bottom-up (Burned Area) inventories

Among the four BB emission inventories selected in this study, FINN1.5 and GFED4s both use the bottom-up method, also known as the Burned Area method. As shown in Table 1, FINN1.5 uses the MODIS (Moderate Resolution Imaging Spectroradiometer) product MCD14DL to calculate the burned area, which can monitor fire points with an area larger than 0.05 km^2. Since the MCD14DL is an active fire detection product that reflects real-time fire point detection, if a fire occurs but the satellite is not in transit or is obscured by clouds while the satellite is in transit, the fire will not be detected (Firms, 2017). Additionally, considering that MODIS on polar-orbiting satellites cannot provide daily coverage products in the tropics (30°N-30°S), FINN1.5 makes some smoothing assumptions for fire detection in this region. It assumes that every fire detected at the equator will continue the next day at half the size of the previous day (Table 1), and this assumption obviously raises some questions (Wiedinmyer et al., 2011; Pan et al., 2020). Meanwhile, the classification of land cover types in FINN1.5 is based on MCD12Q1 (IGBP, version 2005). According to the IGBP land cover classification, each fire is initially assigned to one of 16 land use/land cover (LULC) classes, and then lumped into six generic categories including tropical forest, temperate forest, boreal forest, savanna and grasslands, woody savannas and shrublands, and cropland (Table S1, Wiedingmyer et al., 2011). The amount of usable biomass that can be burned per fire (fuel loadings) for each generic LULC according to Hoelzemann et al. (2004). The FB for each fire is specified as a function of vegetation cover (MODIS Vegetation Continuous Fields (VCF) product), as described by Wiedinmyer et al. (2006; 2011). Emission factors (EFs) for various gaseous and particulate species are determined from a dataset compiled by Akagi et al. (2011) and Andreae and Merlet (2001), and these EFs vary for different LULC types. Currently, FINN1.5 provides the daily global emissions from biomass burning since 2002, including 41 species, with a spatial resolution of 1 km^2 (Table 1).

The main difference between FINN1.5 and GFED4s is that the latter mainly uses MCD64A1 Collection 5.1 burned area product (Giglio et al., 2013; Randerson et al., 2018), which can only detect fires with a size larger than 500 m × 500 m. For small fire burning areas, GFED4s additionally incorporate active fire detection products (MOD14A1 and MYD14A1), and by comparing the difference normalized burned area (dNBR) of active fire products observed inside and outside the 500 m burning area, which compensates to some extent for the bias caused by the lower spatial resolution of the original product MCD64A1 (van der Werf et al., 2017). Note that, according to van der Werf et al. (2017), only small or moderate angel fire point detections are retained in order to reduce uncertainty in geolocation. In general, burned area products reduce uncertainty in fire detection due to satellite non-transit and cloud/smoke obscuration when burn occurs by identifying day-to-day surface variations, such as charcoal and ash deposition, vegetation migration and changes in vegetation structure (Boschetti et al., 2019). According to the annual MODIS MCD12C1 version 5.1 land cover type product and University of Maryland (UMD) classification scheme (Friedl et al., 2010), each fire is also initially assigned to one of 16 LULC subcategories and then lumped into six categories: tropical forest, temperate forest, boreal forest, savanna, cropland (agriculture), and peatland as shown in Table S1. While GFED4s combines the "savanna and grasslands" and "woody savannas and shrublands" in FINN1.5 into one biome, it has an additional biome "peatland". GFED4s generate the fuel loadings and the fraction of biomass burned for each category by combining the burned area and vegetation morality in a modified Carnegie-Ames-Stanford Approach (CASA) model, which is driven by the data of temperature, precipitation, solar radiation, NDVI, and vegetation types (Schaefer et al., 2008; van der Werf et al., 2010; 2017). Additionally, EFs for various gaseous and particulate species follow Akagi et al. (2011) and Andreae and Merlet (2001), also vary with different biome categories. Currently, GFED4s provides the daily global emissions from biomass burning since 1997, including 27 species, with a spatial resolution of 0.25° × 0.25° (Table 1). However, since 2017, the DM provided by GFED4s is derived from a linear relationship between past emissions and MODIS FRP data for the period 2003-2016.

S1.2 Top-down (Fire Radiative Power) inventories

The other two emission inventories selected for this study, QFED2.5 and VFEI0, use a top-down approach, also known as the Fire Radiative Power (FRP) method. Unlike the bottom-up approach, the top-down approach is not based on fire point detection, but on satellite products that detected fire radiated power. QFED2.5 use MODIS Collection 6 MOD14/MYD14 level 2 products to estimate the fire radiative power, and use MOD03/MYD03 to pinpoint the location of the fire (Darmenov and Silva 2015; Liu et al., 2020b). Since MOD14 and MYD14 products are strongly influenced by clouds, missing FRPs are corrected using the "sequential approach" combining current observations and predicted values (Darmenov and da Silva, 2015). The FRPs are then integrated in time to obtain the fire radiative energy (FRE), which is detected and converted to DM by an empirical coefficient α. The initial value of α in QFED2.5 is taken from Kaiser et al. (2009) and subsequently adjusted monthly based on global emissions of GFED2 in 2003–2007, resulting in two sets of empirical coefficients: $\alpha_{MOD14} = 1.89 \times 10^{-6}$ kg (DM) J^{-1} and $\alpha_{MYD14} = 0.644 \times 10^{-6}$ kg (DM) J^{-1}. In QFED2.5, the International Geosphere-Biosphere Programme (IGBP-INPE) dataset classes are used to aggregate 17 land cover classes to four broad vegetation types, including tropical forest, extra-tropical forest (forest classes that exclude tropical forest), savanna, and grassland (Table S1, Darmenov and da Silva 2015). The EFs of particulate or trace gas species are from previous studies (Andreae and Merlet, 2001; Akagi et al., 2011). It is important to note that QFED2.5 scales up the EFs for emissions associated with the particulate phase, such as organic carbon (OC), black carbon (BC), ammonia (NH_3), sulfur dioxide (SO_2), and particulate matter diameter < 2.5μm ($PM_{2.5}$), so emissions of these species are greater in QFED2.5 than in other inventories. The QFED2.5 product covers daily emission inventories from 2000 to the present, and contains 17 emission species with a spatial resolution of up to 0.1° × 0.1°.

VFEI0 also adopts the top-down method but uses VNP14IMG.001 FRP product from VIIRS I-band (Visible Infrared Imaging Radiometer), which can detect smaller and colder flames than MODIS (1 km resolution at nadir), since it has a resolution of 375 m at nadir (Ferrada et al., 2022). Unlike QFED2.5, VFEI0 has no cloud calibration, but it will be supplemented in future versions. It also uses the empirical coefficient α to convert the detected FRE into DM, but α is derived from the linear regression of GFED3.1DM and VIIRS FRP. Additionally, MCD12C1 (IGBP, version 2015) is the underlying LULC data, which is further supplemented by Köppen climate classification (Beck et al., 2018) to define ten subcategories in VFEI0 (i.e., Tropical forest, Savanna, Temperate forest, Temperate Savanna, Boreal forest, Boreal Savanna, Grass, Agriculture, Peatland and Desertic areas). VFEI0 then grouped the previous ten subcategories into six biomes (Table S1), corresponding to the emission factors provided by Andreae (2019), to calculate the BB emission inventory. Among the four BB emission inventories, VFEI0 provides the shortest inventory time coverage (daily emission fluxes from 20 January 2012 to the present), but it provides the largest number of emitted species at 46 and the highest horizontal resolution of 0.005° × 0.005° (Table 1).

References:

Andreae, M. O. and Merlet, P.: Emission of trace gases and aerosols from biomass burning, Global biogeochemical cycles, 15, 955-966, 2001.

Andreae, M. O.: Emission of trace gases and aerosols from biomass burning–an updated assessment, Atmospheric Chemistry and Physics, 19, 8523-8546, 2019.

Akagi, S., Yokelson, R. J., Wiedinmyer, C., Alvarado, M., Reid, J., Karl, T., Crounse, J., and Wennberg, P.: Emission factors for open and domestic biomass burning for use in atmospheric models, Atmospheric Chemistry and Physics, 11, 4039-4072, 2011.

Beck, H. E., Zimmermann, N. E., McVicar, T. R., Vergopolan, N., Berg, A., and Wood, E. F.: Present and future Köppen-Geiger climate classification maps at 1-km resolution, Scientific data, 5, 1-12, 2018. Bian, H., Chin, M., Kawa, S., Duncan, B., Arellano, A., and Kasibhatla, P.: Sensitivity of global CO simulations to uncertainties in biomass burning sources, Journal of Geophysical Research: Atmospheres, 112, 2007.

Boschetti, L., Roy, D. P., Giglio, L., Huang, H., Zubkova, M., and Humber, M. L.: Global validation of the collection 6 MODIS burned area product, Remote sensing of environment, 235, 111490, 2019.

Firms, L.: Collection 6 NRT hotspot/active fire detections MCD14DL, En ligne: https://earthdata. nasa. gov/firms (visité le 21 June 2017), 2017.

Darmenov, A., da Silvia, A., and Koster, R.: The Quick Fire Emissions Dataset (QFED): Documentation of Versions 2.1, 2.2 and 2.4. Volume 38; Technical Report Series on Global Modeling and Data Assimilation, 2015.

Ferrada, G. A., Zhou, M., Wang, J., Lyapustin, A., Wang, Y., Freitas, S. R., and Carmichael, G. R.: Introducing the VIIRS-based Fire Emission Inventory version 0 (VFEIv0), Geoscientific Model Development, 15, 8085-8109, 2022.

Friedl, M. A., Sulla-Menashe, D., Tan, B., Schneider, A., Ramankutty, N., Sibley, A., and Huang, X.: MODIS Collection 5 global land cover: Algorithm refinements and characterization of new datasets, Remote sensing of Environment, 114, 168-182, 2010.

Giglio, L., Randerson, J. T., and van der Werf, G. R.: Analysis of daily, monthly, and annual burned area using the fourth-generation global fire emissions database (GFED4), Journal of Geophysical Research: Biogeosciences, 118, 317-328, 2013.

Hoelzemann, J. J., Schultz, M. G., Brasseur, G. P., Granier, C., and Simon, M.: Global Wildland Fire Emission Model (GWEM): Evaluating the use of global area burnt satellite data, Journal of Geophysical Research: Atmospheres, 109, 2004.

Kaiser, J., Flemming, J., Schultz, M., Suttie, M., and Wooster, M.: The MACC global fire assimilation system: First emission products (GFASv0), Tech. Memo. 596, ECMWF, Reading, UK, 2009.

Kaiser, J., Heil, A., Andreae, M., Benedetti, A., Chubarova, N., Jones, L., Morcrette, J.-J., Razinger, M., Schultz, M., and Suttie, M.: Biomass burning emissions estimated with a global fire assimilation system based on observed fire radiative power, Biogeosciences, 9, 527-554, 2012.

Liu, T., Mickley, L. J., Marlier, M. E., DeFries, R. S., Khan, M. F., Latif, M. T., and Karambelas, A.: Diagnosing spatial biases and uncertainties in global fire emissions inventories: Indonesia as regional

case study, Remote Sensing of Environment, 237, 111557, 2020b.
Pan, X., Ichoku, C., Chin, M., Bian, H., Darmenov, A., Colarco, P., Ellison, L., Kucsera, T., da Silva, A., and Wang, J.: Six global biomass burning emission datasets: intercomparison and application in one global aerosol model, Atmospheric Chemistry and Physics, 20, 969-994, 2020.
Randerson, J. T., van der Werf, G. R., Giglio, L., Collztz, G. J., and Kasibhatla, P. S.: Global Fire Emission Database, Version 4.1 (GFEDv4). ORNLDAAC, Oak Ridge, Tennessee, USA, 2018. https://doi.org/10.3334/ORNLDAAC/1293.
Schaefer, K., Collatz, G. J., Tans, P., Denning, A. S., Baker, I., Berry, J., Prihodko, L., Suits, N., and Philpott, A.: Combined simple biosphere/Carnegie-Ames-Stanford approach terrestrial carbon cycle model, Journal of Geophysical Research: Biogeosciences, 113, 2008.
van der Werf, G. R., Randerson, J. T., Giglio, L., van Leeuwen, T. T., Chen, Y., Rogers, B. M., Mu, M., van Marle, M. J., Morton, D. C., and Collatz, G. J.: Global fire emissions estimates during 1997–2016, Earth System Science Data, 9, 697-720, 2017.
van der Werf, G. R., Randerson, J. T., Giglio, L., Collatz, G., Mu, M., Kasibhatla, P. S., Morton, D. C., DeFries, R., Jin, Y. v., and van Leeuwen, T. T.: Global fire emissions and the contribution of deforestation, savanna, forest, agricultural, and peat fires (1997–2009), Atmospheric chemistry and physics, 10, 11707- 11735, 2010.
van der Werf, G. R., Randerson, J. T., Giglio, L., van Leeuwen, T. T., Chen, Y., Rogers, B. M., Mu, M., van Marle, M. J., Morton, D. C., and Collatz, G. J.: Global fire emissions estimates during 1997–2016, Earth System Science Data, 9, 697-720, 2017.
Wiedinmyer, C., Akagi, S., Yokelson, R. J., Emmons, L., Al-Saadi, J., Orlando, J., and Soja, A.: The Fire INventory from NCAR (FINN): A high resolution global model to estimate the emissions from open burning, Geoscientific Model Development, 4, 625-641, 2011.
Wiedinmyer, C., Quayle, B., Geron, C., Belote, A., McKenzie, D., Zhang, X., O’Neill, S., and Wynne, K. K.: Estimating emissions from fires in North America for air quality modeling, Atmospheric Environment, 40, 3419-3432, 2006.

Table S1. LULC classifications and seven generic land cover classes as assigned by four BB datasets.

	LCT	FINN1.5	GFED4s	QFED2.5	VFEI0
Tropical	Evergreen Broadleaf Forest	Tropical forest	Tropical forest	Tropical forest	Tropical forest
	Closed Shrublands	Tropical forest	Tropical forest	Tropical forest	Tropical savanna
	Open Shrublands	Savanna	Savanna	Savanna	Tropical savanna
	Woody Savanna	Tropical forest	Tropical forest	Tropical forest	Tropical savanna
	Savanna	Savanna	Savanna	Savanna	Tropical savanna
Temperate	Evergreen Needleleaf Forest	Boreal forest	Extratropical forest(50-70° N Boreal forest)	Extratropical forest	Temperate forest
	Evergreen Broadleaf Forest	Tropical forest	Temperate forest	Temperate forest	Temperate forest
	Deciduous Needleleaf Forest	Boreal forest	Extratropical forest(50-70° N Boreal forest)	Extratropical forest	Temperate forest
	Deciduous Broadleaf Forest	Temperate forest	Extratropical forest(50-70° N Boreal forest)	Extratropical forest	Temperate forest
	Mixed Forest	Temperate forest	Extratropical forest(50-70° N Boreal forest)	Extratropical forest	Temperate forest
	Closed Shrublands	Temperate forest	Extratropical forest(50-70° N Boreal forest)	Extratropical forest	Temperate savanna
	Open Shrublands	Savanna	Savanna	Savanna	Temperate savanna
	Woody Savanna	Temperate forest	Extratropical forest(50-70° N Boreal forest)	Extratropical forest	Temperate savanna
	Savanna	Savanna	Savanna	Savanna	Temperate savanna
Boreal	Evergreen Needleleaf Forest	Boreal forest	Extratropical forest(50-70° N Boreal forest)	Extratropical forest	Boreal forest
	Deciduous Needleleaf Forest	Boreal forest	Extratropical forest(50-70° N Boreal forest)	Extratropical forest	Boreal forest
	Mixed Forest	Temperate forest	Extratropical forest(50-70° N Boreal forest)	Extratropical forest	Boreal forest
	Closed Shrublands	Boreal forest	Extratropical forest(50-70° N Boreal forest)	Extratropical forest	Boreal savanna
	Open Shrublands	Savanna	Savanna	Savanna	Boreal savanna
	Woody Savanna	Boreal forest	Extratropical forest	Extratropical forest	Boreal savanna
	Savanna	Savanna	Savanna	Savanna	Boreal savanna
	Grasss	Savanna	Grass	Grass	Grass
	Urban and Built-Up	bare	Grass	Grass	Grass
	Crops	Crop	Crop	Grass	Crop
	Crop/Natural Vegetation Mosaic	Grass	Crop	Grass	Crop
	Permanent Wetlands	Grass	Peatland	Grass	Peatland
	Snow and Ice	bare	Grass	Grass	Desertic areas
	Barren or Sparsely Vegetated	Grass	Grass	Grass	Desertic areas

Tropical forest
Temperate forest
Boreal forest
Extratropical forest
Savanna and Grass
Crop
Peatland

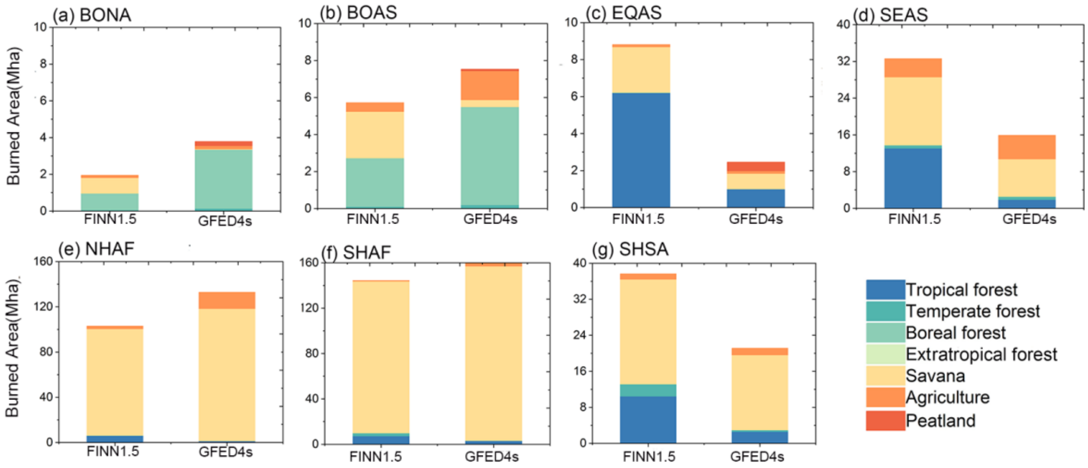

Figure S1. Burned area of two bottom-up datasets (namely FINN1.5 and GFED4s) across seven regions during 2013-2016.

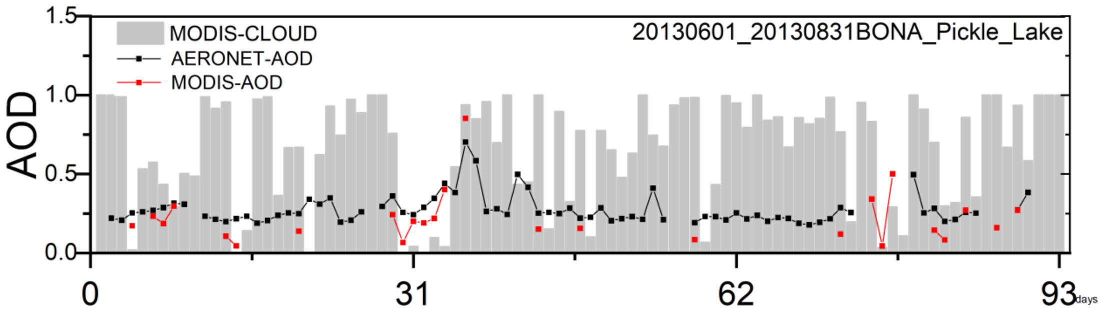

Figure S2. The time series of MODIS AOD, MODIS cloud fractions and AERONET ground-based observations during the combustion at Pickle Lake station in BONA. It shows that there are more missing detections in MODIS (red dots), which directly demonstrates that clouds will block the observations of MODIS.

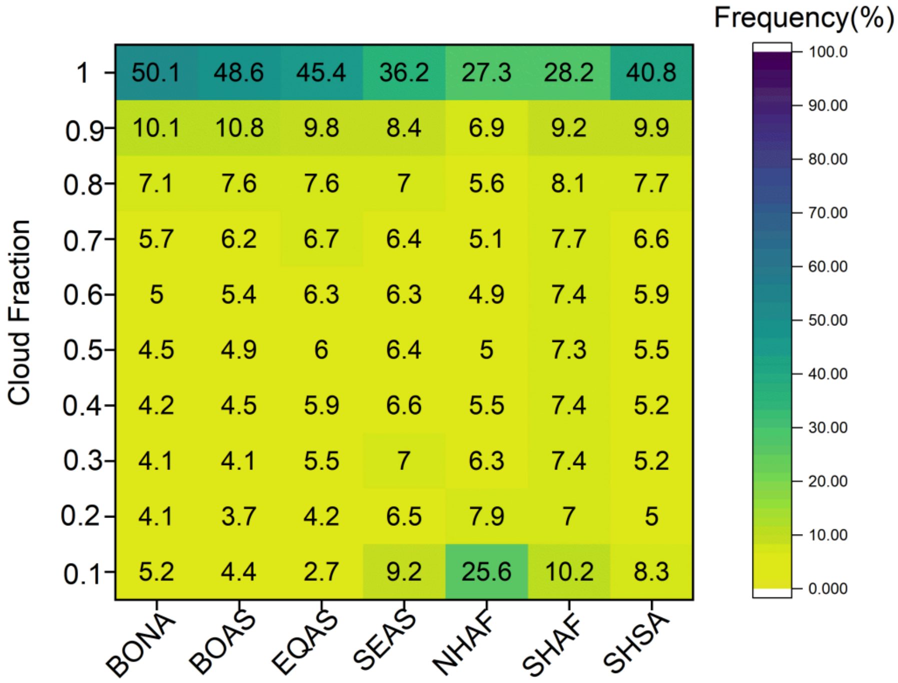

Figure S3. Annual mean frequency of different cloud fractions across seven BB regions from 2013 to 2016.

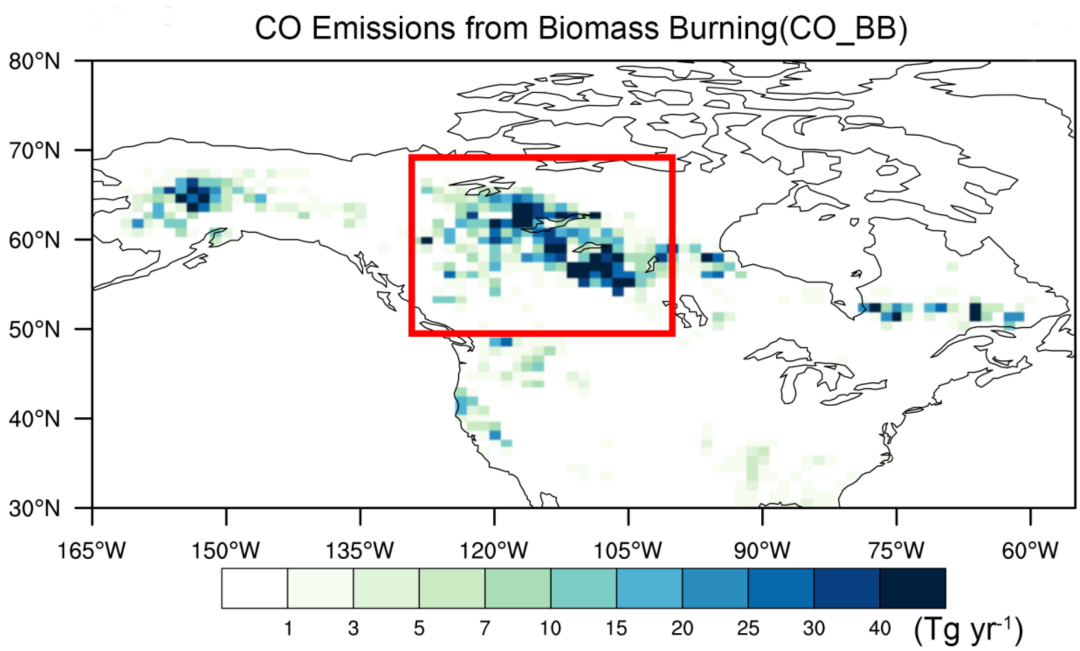

Figure S4. The spatial distribution of CO emissions in BONA, and the region with high BB emissions is marked with red box, namely Alberta and Saskatchewan in Canada within 50°E - 70°E and 100°W-130°W.

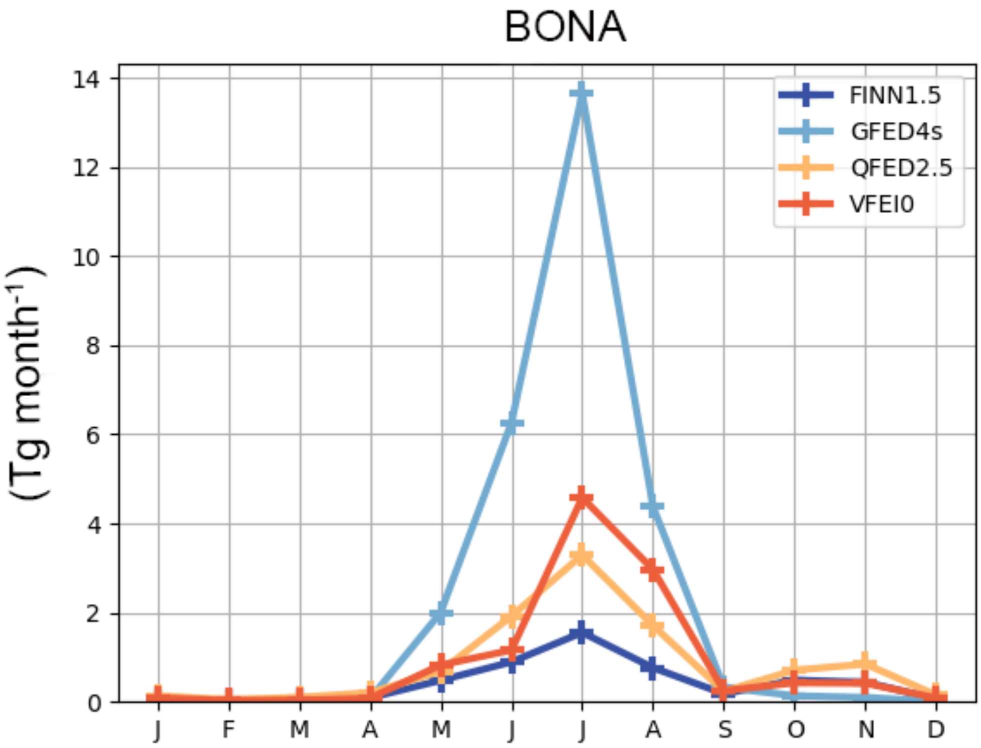

Figure S5. Monthly variation of CO biomass burning emissions in BONA among four BB datasets, mean values from 2013 to 2016 were used.

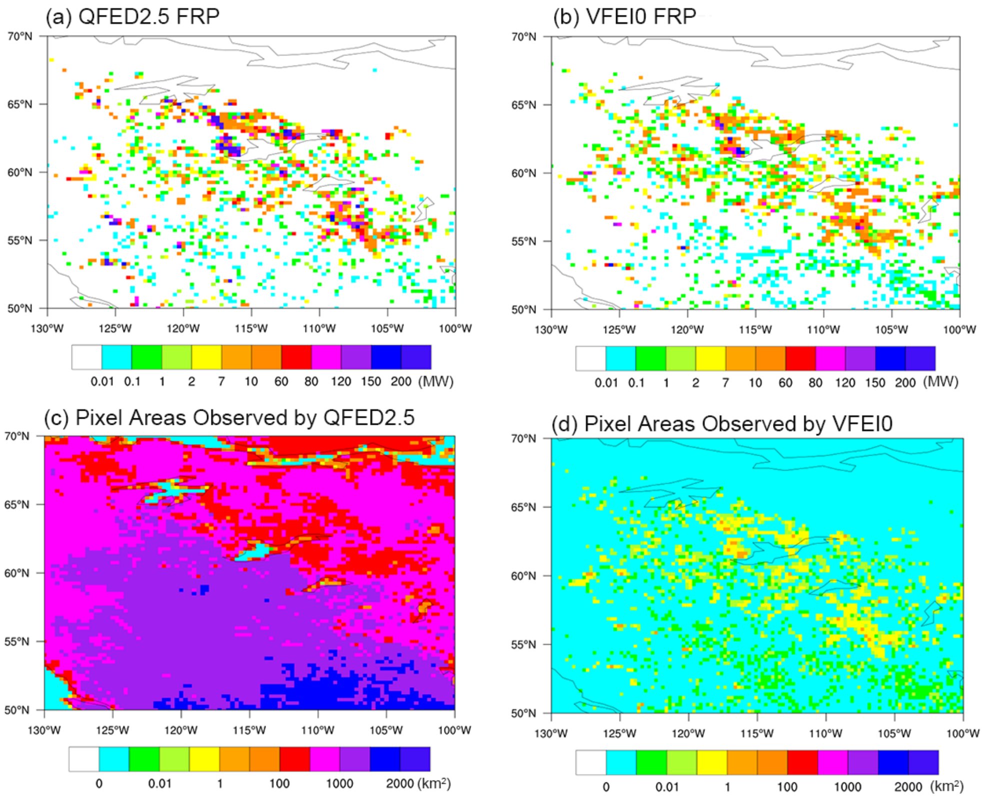

Figure S6. (a-b) Distribution of FRP and (c-d) satellite pixel area of QFED2.5 and VFEI0 in the region shown in Figs. 5 during each July from 2013 to 2016. In this study we use the mean FRP of MOD and MYD for QFED2.5 since the VFEI0 FRP is the average between day and nighttime observations.

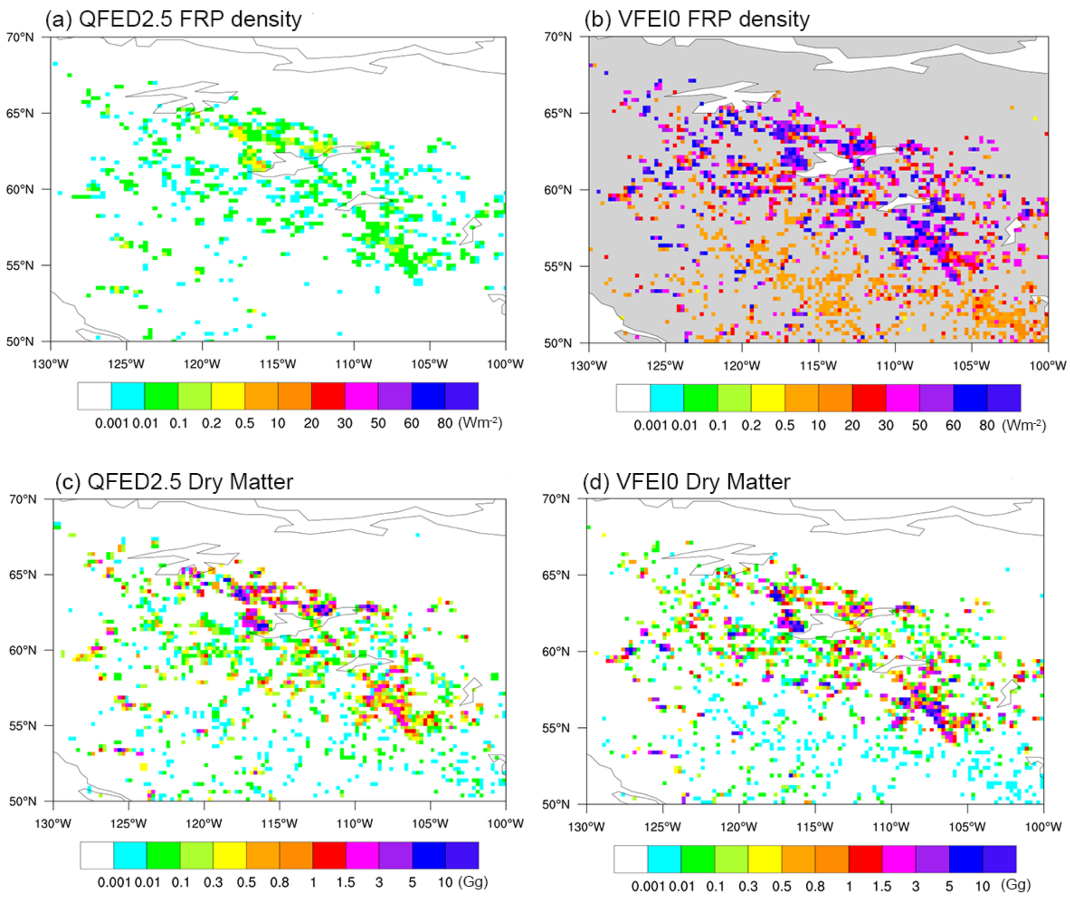

Figure S7. (a-b) Distribution of FRP density and (c-d) final DM in QFED2.5 and VFEI0 in the region shown in Figs. 5 during each July from 2013 to 2016.